Supplement of Atmos. Chem. Phys., 22, 14879–14891, 2022
https://doi.org/10.5194/acp-22-14879-2022-supplement

Atmospheric Chemistry and Physics
Open Access

Supplement of

Vertical profiles of cloud condensation nuclei number concentration and its empirical estimate from aerosol optical properties over the North China Plain

Rui Zhang et al.

Correspondence to: Yuying Wang (yuyingwang@nuist.edu.cn)

Table S1. The fitting results of Eq. (1) for the 11 level flights

Flight code	Altitude (km)	*C*	*k*	R^2
RF1_a	3.6	156	0.18	0.59
RF2_a	0.4	3029	1.71	0.94
RF2_b	3.6	2317	0.86	0.88
RF2_c	0.4	6560	1.75	0.92
RF6_a	2.5	282	0.46	0.91
RF6_b	1.1	9981	0.79	0.83
RF7_a	3.1	391	0.62	0.95
RF7_b	0.4	3218	0.65	0.73
RF7_c	1.8	828	0.37	0.91
RF8_a	0.6	8120	0.89	0.91
RF11_a	0.7	10310	0.97	0.96

Sampling method

The sampling device is above the front of the airplane cabin, which is not affected by the propeller after the plane takes off. The sampling flow was iso-kinetic. As described in Wang et al. (2018), the conical double diffuser aerosol inlet, designed for a Twin Otter, is installed on the Y-12. This inlet system is manufactured by Droplet Measurements Technologies (MP-1806-A and MP-1807-A, Boulder, CO, USA) (Hegg et al., 2005). The passing efficiency is expected to be near 100% for particle diameters up to 2.5 μm and near 50% for particles between 3 and 4 μm (Huebert et al., 2004; McNaughton et al., 2007). The typical cruising speed of aircraft is 60-70 m s^{-1}, with ascent/descent rates of 2–5 m s^{-1}. Ascents and descents are gentle to avoid turbulence taking about 20 min to ascend 3000 m or ~150 m/min. The ram heating is considered by adjusting the measured air temperature and relative humidity:

$$Temp\_adj = (Temp + 273.15) / (1 + 0.2 * Rf * M^2) - 273.15,$$

where,

Temp_adj – adjusted air temperature by taking the ram heating effect into account

Temp – measured air temperature (°C)

Rf – recovery factor (rf = 0.896445604404384)

M – mach number, which is calculated from the measured true air speed and calculated speed of sound:

$$M = Airspeed\_True / Speed\_sound$$

$$Speed\_sound = 331.3 * sqrt ((Temp + 273.15) /273.15)$$

Relative humidity is also adjusted by multiplying the ratio of saturated water pressures under measured and adjusted air temperature:

$$RH\_adj=RH*(svpt/svpat);$$

where,

$svpt=6.1121 * exp ((18.678 – Temp / 234.5) * (Temp / (257.14 + Temp)));$

$svpat=6.1121 * exp ((18.678 - Temp\_adj / 234.5) * (Temp\_adj / (257.14 + Temp\_adj)))$

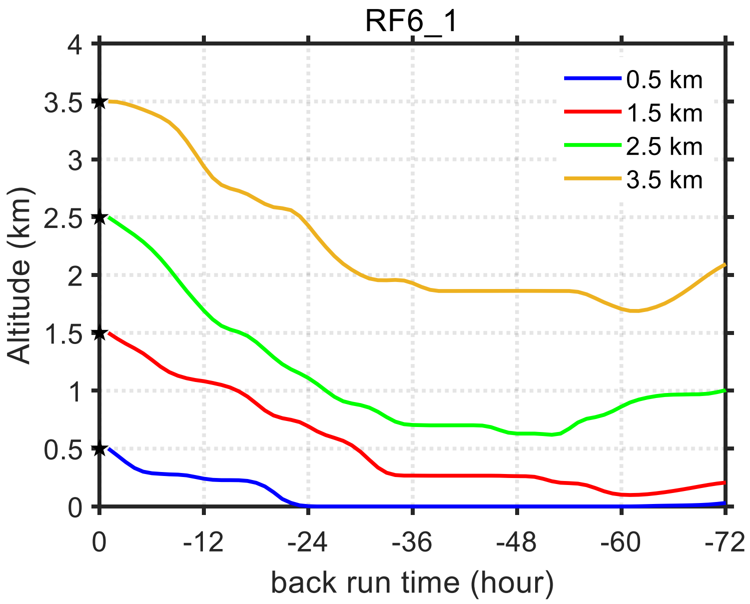

Figure S1. Seventy-two-hour HYSPLIT back trajectories in southeasterly air masses at 0.5, 1.5, 2.5, and 3.5 km starting altitudes (showing RF6_1 as the example).

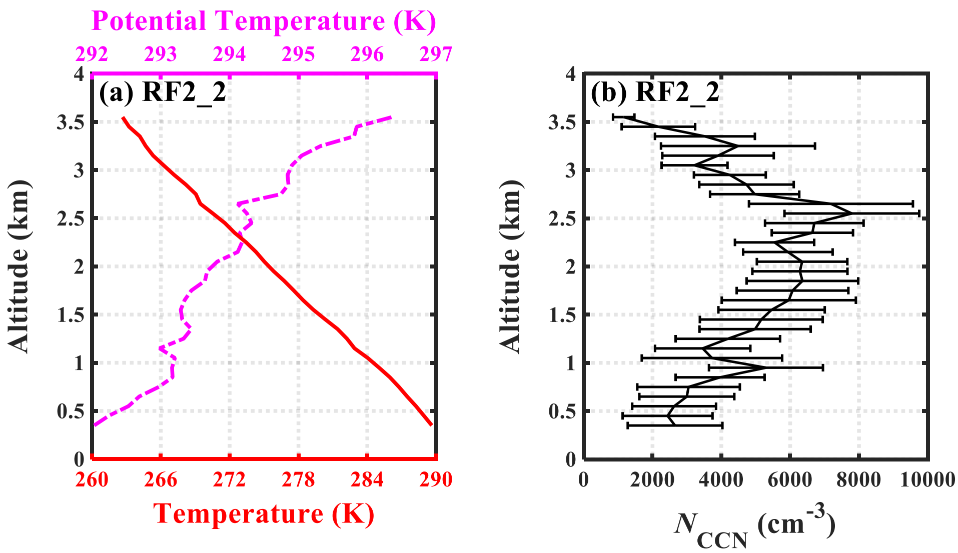

Figure S2. Same as Fig. 3 but for RF2_2 N_{CCN} profile with no TIL.

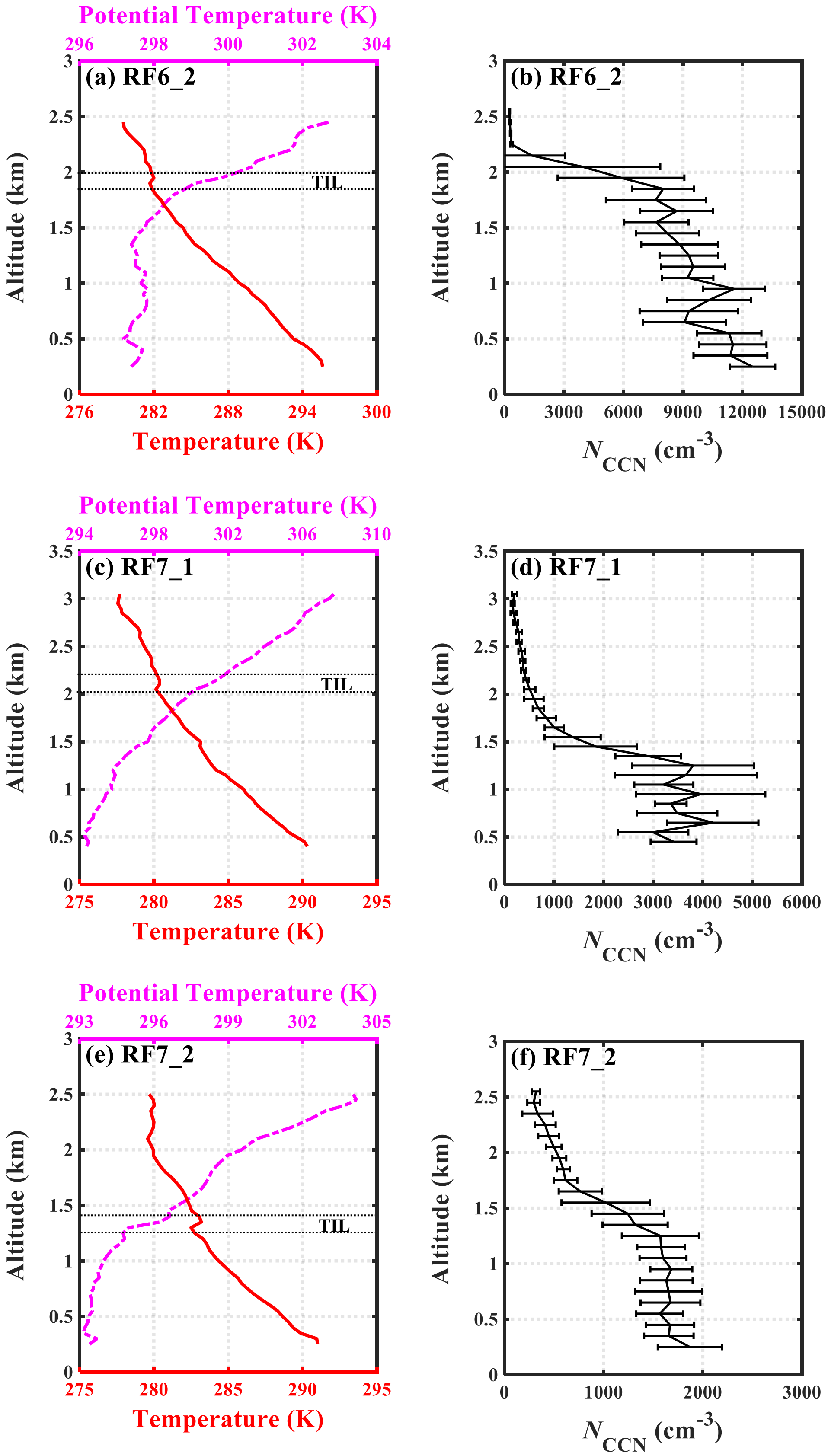

Potential Temperature (K)
(a) RF6_2
TIL
Altitude (km)
Temperature (K)
(b) RF6_2
N CCN (cm-3)
(c) RF7_1
(d) RF7_1
(e) RF7_2
(f) RF7_2

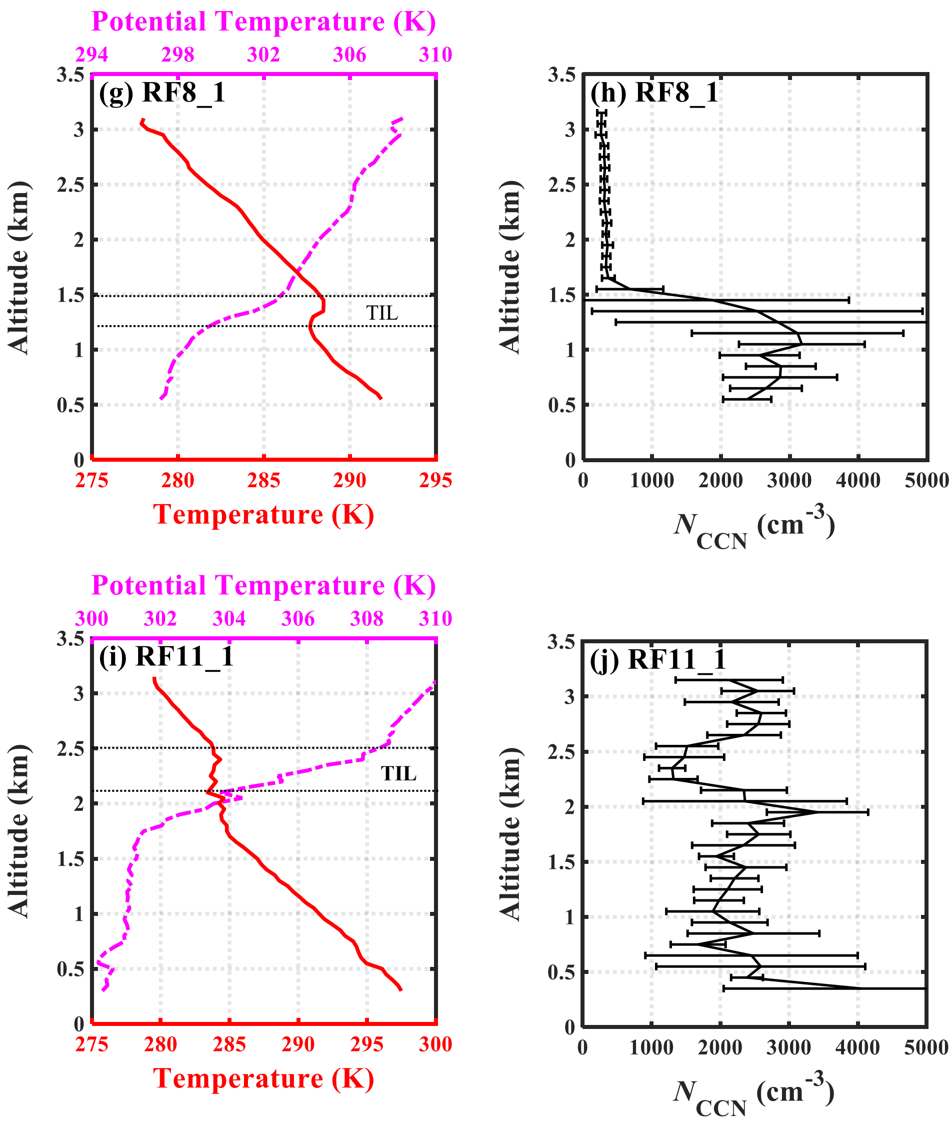

Figure S3. Same as Fig.3 but for RF6_2, RF7_1, RF7_2, RF8_1, and RF11_1 N_{CCN} profiles with one TIL.

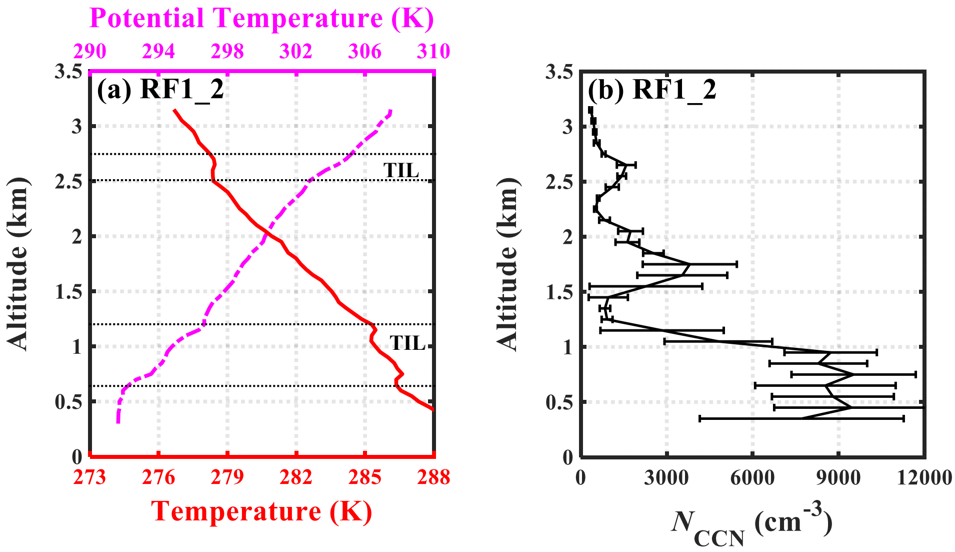

Figure S4. Same as Fig.3 but for RF1_2 N_{CCN} profiles with dual TIL.

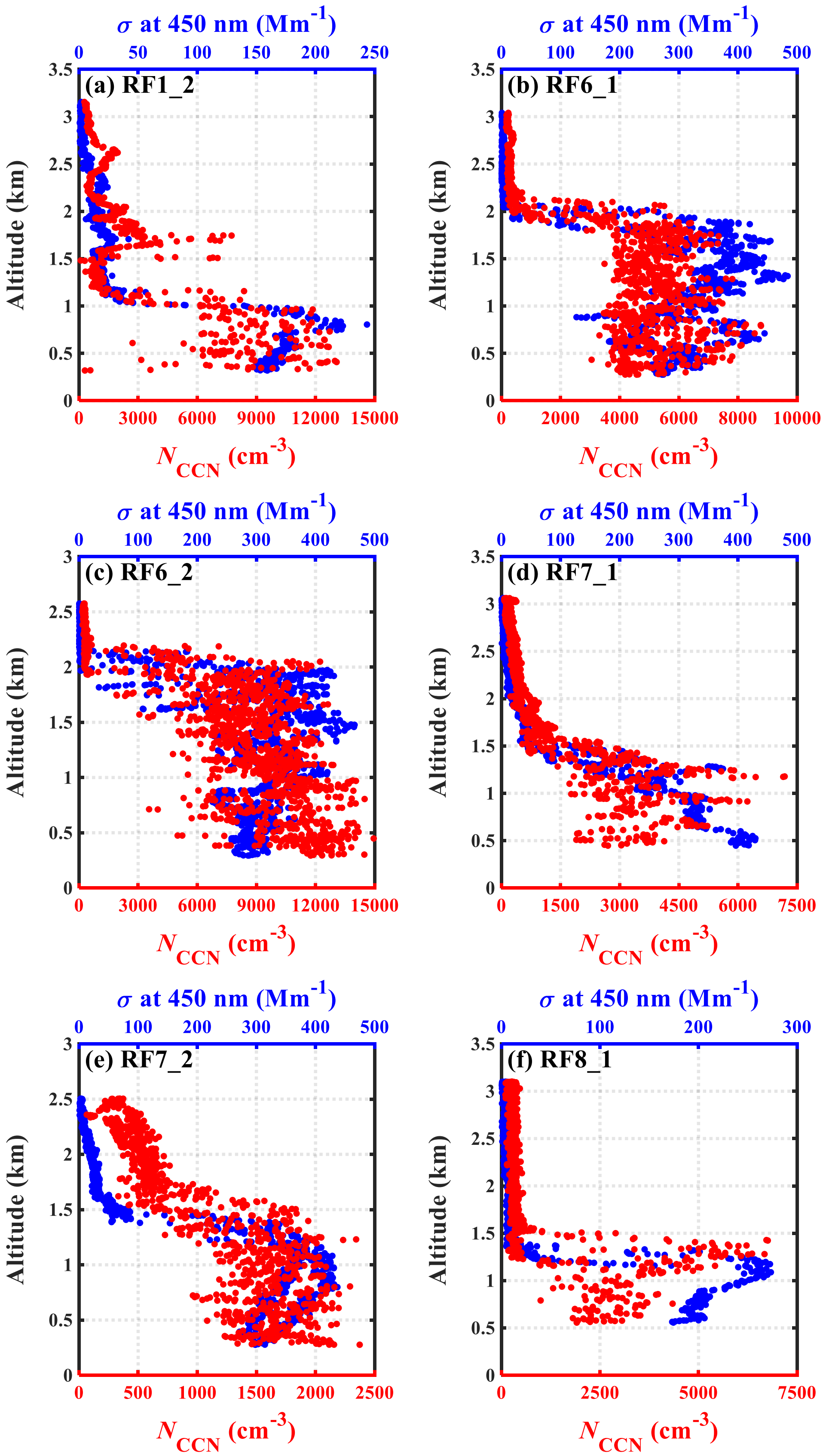

Figure S5. Same as Fig. 6b but in (**a**) RF1_2, (**b**) RF6_1, (**c**) RF6_2, (**d**) RF7_1, (**e**) RF7_2, and (**f**) RF8_1 vertical spiral flight.

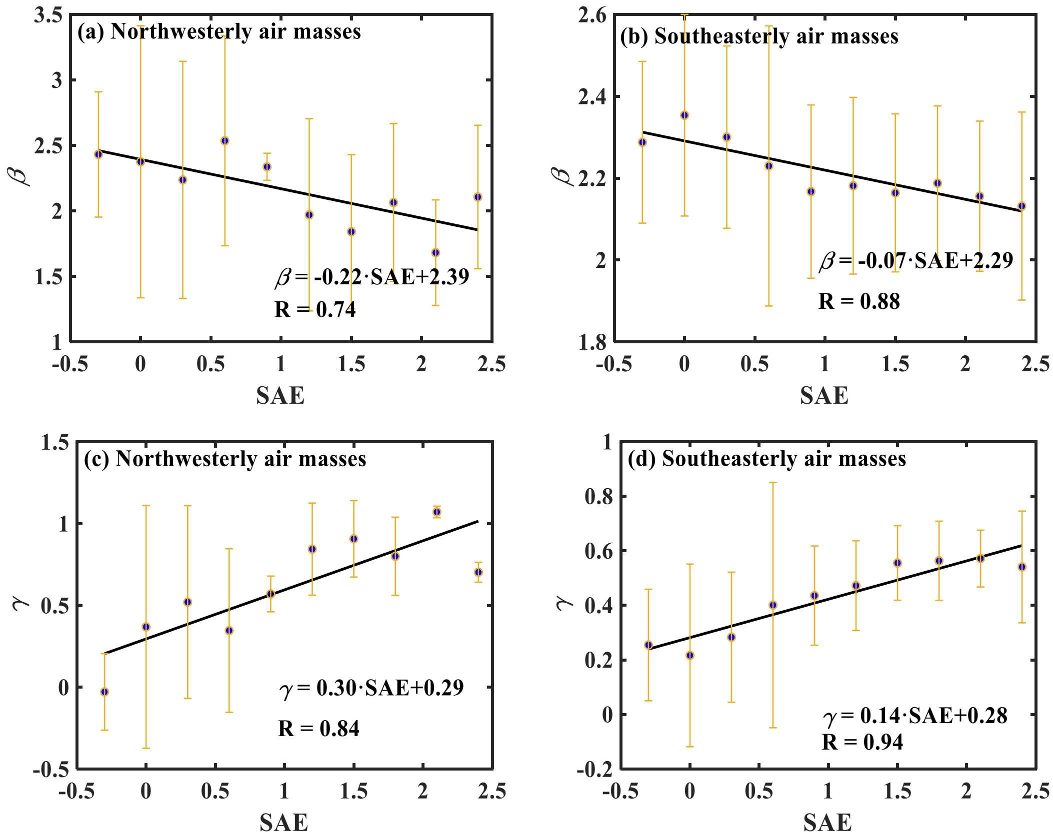

Figure S6. The two fitting parameters β and γ as a function of the aerosol scattering Ångström exponent (SAE) in northwesterly air masses (**a** and **c**) and southeasterly air masses (**b** and **d**). The dots are mean values averaged in 0.3-wide SAE bins. The black lines are best-fit lines from linear regression. Linear relations and correlation coefficients are given in each panel. The yellow error bars denote standard deviations.

Reference:

Hegg, D. A., Covert, D. S., Jonsson, H., and Covert, P. A.: Determination of the transmission efficiency of an aircraft aerosol inlet, Aerosol Sci. Technol., 39, 966–971, https://doi.org/10.1080/02786820500377814, 2005.

Huebert, B., Bertram, T., Kline, J., Howell, S., Eatough, D., and Blomquist, B.: Measurements of organic and elemental carbon in Asian outflow during ACE-Asia from the NSF/NCAR C-130, J. Geophys. Res.-Atmos., 109, D19S11, https://doi.org/10.1029/2004JD004700, 2004.

McNaughton, C. S., Clarke, A. D., Howell, S. G., Pinkerton, M., Anderson, B., Thornhill, L., Hudgins, C., Winstead, E., Dibb, J. E., and Scheuer, E.: Results from the DC-8 Inlet Characterization Experiment (DICE): Airborne versus surface sampling of mineral dust and sea salt aerosols, Aerosol Sci. Technol., 41, 136–159, https://doi.org/10.1080/02786820601118406, 2007.

Wang, F., Li, Z., Ren, X., Jiang, Q., He, H., Dickerson, R. R., Dong, X., and Lv, F.: Vertical distributions of aerosol optical properties during the spring 2016 ARIAs airborne campaign in the North China Plain, Atmos. Chem. Phys., 18, 8995-9010, https://doi.org/10.5194/acp-18-8995-2018, 2018.